



Interactions between potassium ashes and oxygen carriers based on natural and waste materials at different initial oxidation states

Downloaded from: <https://research.chalmers.se>, 2025-12-04 17:04 UTC

Citation for the original published paper (version of record):

Purnomo, V., Hildor, F., Knutsson, P. et al (2023). Interactions between potassium ashes and oxygen carriers based on natural and waste materials at different initial oxidation states. *Greenhouse Gases: Science and Technology*, 13(4): 520-534.
<http://dx.doi.org/10.1002/ghg.2208>

N.B. When citing this work, cite the original published paper.

Interactions between potassium ashes and oxygen carriers based on natural and waste materials at different initial oxidation states

Victor Purnomo, Fredrik Hildor, Pavleta Knutsson and Henrik Leion, Division of Energy and Materials, Department of Chemistry and Chemical Engineering, Chalmers University of Technology, Göteborg, Sweden

Abstract: One of the most essential features of an oxygen carrier is its ability to be oxidized and reduced in order to transfer oxygen in a chemical looping system. A highly reduced oxygen carrier can experience multiple performance issues, such as decreased reactivity, agglomeration, and defluidization. This is crucial for processes that require limited oxygen transfer from the air reactor to the fuel reactor. Meanwhile, biomasses as environmentally friendly fuel options contain ashes, which would inevitably react with oxygen carriers and exacerbate the performance issues. To mimic the interactions between a highly reduced oxygen carrier and biomass ash compounds, four iron-based oxygen carriers, based on natural ores and waste materials, and three potassium salts, K_2CO_3 , KH_2PO_4 , and K_2SO_4 , were investigated in a tubular reactor under an atmosphere consisting of 2.5% H_2 and 10% steam in Ar and N_2 at 900°C for 3 h. The results from the X-ray diffraction (XRD) material analysis showed that both initially fully oxidized and highly reduced materials reach the same oxidation state after the experiment. Based on the scanning electron microscopy coupled with energy dispersive X-ray spectroscopy results, K from K_2CO_3 and K_2SO_4 diffuses in the oxygen carrier particles, while K from KH_2PO_4 always forms a distinct layer around the particles. The initial oxidation state of an oxygen carrier surface affects the interactions with the potassium salt only to minor extents. Thus, the final state of the material and its performance in a large-scale process are only occasionally and mildly affected by its initial oxidation state. © 2023 The Authors. *Greenhouse Gases: Science and Technology* published by Society of Chemical Industry and John Wiley & Sons Ltd.

Additional supporting information may be found online in the Supporting Information section at the end of the article.

Keywords: biomass ash; chemical looping; initial oxidation state; interactions; oxygen carrier; potassium salts

Correspondence to: Victor Purnomo, Division of Energy and Materials, Department of Chemistry and Chemical Engineering, Chalmers University of Technology, Göteborg, 412 58, Sweden.

Email: purnomo@chalmers.se

Received January 31, 2023; revised February 28, 2023; accepted February 28, 2023

Published online at Wiley Online Library (wileyonlinelibrary.com). DOI: 10.1002/ghg.2208

This is an open access article under the terms of the Creative Commons Attribution License, which permits use, distribution and reproduction in any medium, provided the original work is properly cited.

Introduction

Oxygen carrier (OC) plays an important role in chemical looping processes, as it is able to transfer heat and oxygen from air reactor (AR) to fuel reactor (FR), hence avoiding the mixing of flue gases and nitrogen from the air. A large number of synthetic metal oxides has been studied and investigated previously. Such oxygen carriers are usually made by impregnating an inert supporting substrate with a desired metal compound, which in its pure form does not have oxygen carrier performance but mechanical and chemical reliability.¹ Among the investigated oxygen carriers, it has been widely known that iron-based materials are easy to obtain, inexpensive, environmentally sound, and, above all, have reasonable reactivity toward fuel.²

Since the production of synthetic oxygen carriers is expensive, it is of utmost importance to be able to find and use a more affordable yet suitable oxygen carrier materials. So far, ilmenite (an iron–titanium ore) has been known as one of the benchmark oxygen carriers.³ This is due to the fact that ilmenite, as well as the other iron-based materials, is abundantly available and easy to obtain in a large amount. Previous studies have also shown that even though ilmenite has average chemical performance,⁴ it has an excellent physical performance as an oxygen carrier in multiple chemical looping pilot plants and even in a commercial oxygen-carrier-aided combustion (OCAC) unit.⁵ Nevertheless, ilmenite also has showed a tendency for defluidization when it comes to a highly reducing environment. Highly reducing conditions can be prevalent in processes such as chemical looping gasification (CLG), a process used among others for production of H_2 and bio-oil.⁶ The same tendency for defluidization has not been observed for copper slag, also known as iron sand,⁷ and steel converter slag (LD slag),⁶ two other iron-based waste materials. This makes them interesting alternatives as oxygen carriers.

Since biomass obtains its carbon content from the atmosphere, the utilization of biomass in chemical looping process would make the process carbon neutral, if not carbon negative.⁸ The latter case is possible with the aid of a carbon capture and storage (CCS) unit, which would be much more efficient and economically viable in the case of chemical looping as the flue gas does not contain nitrogen. However, the ash compounds in biomass will inevitably interact with the oxygen carrier materials.⁹ This can result in

performance issues in both oxygen-carrier-aided combustion (OCAC)¹⁰ and chemical looping units.¹¹ Stanić et al.⁹ suggested that K_2CO_3 caused severe agglomeration on two iron-based oxygen carriers. Störner et al.¹² found that K_2CO_3 affected the reactivity of mill scale and steel converter slag and KH_2PO_4 did cause agglomeration of both aforementioned oxygen carriers. Yilmaz et al.¹³ reported serious agglomeration of oxygen carriers when they are exposed to either $CaCO_3$, $Ca(NO_3)_2$, $Ca_3(PO_4)_2$, or the equivalent Mg-based salts. Cheng et al.¹⁴ observed sintering and decreased oxygen-releasing performance of iron-based oxygen carriers in a fixed bed reactor when Ca^{2+} , K^+ , and Na^+ ions from biomass ashes reacted with the oxygen carriers. Rubel et al.¹⁵ observed an increased oxygen take-up on two different iron-based oxygen carriers when iron-containing ash compounds were added. Furthermore, Bao et al.¹⁶ reported that the impregnation of K^+ increased the reduction reactivity of ilmenite. Despite having addressed different ash compounds and their interaction with the oxygen carrier, none of the previous studies has reported the effect of the initial oxidation state of an oxygen carrier on the interactions between an ash compound and the material, especially when the material is initially highly reduced.

This study aims to bring forward the laboratory-based findings on how potassium salts, which represent relevant compounds in biomass ashes, may interact with initially highly reduced iron-based oxygen carriers. As a comparison, the same oxygen carriers were also prepared in a fully oxidized state. It should be noted that this study is largely qualitative since the aim is to enhance the knowledge on the physical interaction between oxygen carriers and ashes. The experiments were designed by mixing an oxygen carrier material with a potassium salt in an alumina crucible at high temperature in a reducing environment. The samples were characterized using X-ray diffraction (XRD) and Scanning Electron Microscopy/Energy-Dispersive X-ray (SEM/EDX).

Materials and methods

Iron-based oxygen carriers and potassium salts

Four iron-based oxygen carriers were investigated in this study, one originating from an ore and three recovered from industrial wastes. Table 1 presents the used oxygen carriers along with their chemical

Table 1. Elemental content of the oxygen carriers (major components) used in this study.

Element	Composition (wt %)			
	Ilmenite ¹⁷	Iron sand ⁷	LD slag ¹⁸	Mill scale ^{* 12}
Fe	34	35	17	95
Mn	0.48	0.35	2.6	0.90
Si	0.15	16	5.6	4.0
Ti	28	0.13	0.78	-
Ca	0.060	2.3	32	-
Al	0.19	2.4	0.76	-

*Analyzed on an oxygen-free basis.

contents. Ilmenite, a benchmark chemical-looping oxygen carrier, is an iron-titanium ore, which was provided by Titania A/S.¹⁷ Iron sand, also known as copper slag, is a by-product from a copper smelting plant run by Boliden AB and contains mainly iron and silicon.⁷ Linz-Donawitz (LD) slag is a by-product from steel manufacturing process, which was obtained from the Swedish steel production company SSAB, and is notable for its calcium content, about 32 wt.%.¹⁸ Mill scale here is a residue product from steel sheets rolling and was also provided by SSAB and comprises mostly iron oxides.¹² The main elemental content of each oxygen carriers is provided in Table 1. Note that the minor constituents are excluded here.

All oxygen carriers were calcined in a high-temperature box furnace at 950°C for 12 h. The calcined oxygen carriers were then sieved into the size range 125–180 μm , which is the suitable particle size range for the batch fluidized bed used in this study.¹⁹ Twenty grams of each sieved oxygen carrier was activated, using the activation procedure described by Schwebel et al.,²⁰ until a stable CO conversion was achieved. This was done in a batch fluidized bed setup at 900°C using 50% CO in N₂ with a flow rate of 600 ml/min (25°C, 1 atm). After activation, each activated material was reduced with the same gas mixture to produce highly reduced oxygen carriers.^{6,7} It should be noted that the oxygen capacity of the oxygen carrier varies, so that two materials may have lost different amount of available oxygen and, hence, different mass conversion degrees when they are considered highly reduced (see Table 2). This is because the amount of available oxygen varies between the examined materials. Mass conversion degree is

Table 2. Mass conversion degree of the oxygen carriers tested in the present study after their reduction in the batch fluidized bed setup.

Oxygen carrier	Mass conversion degree (ω)
Ilmenite	0.96
Iron sand	0.99
LD slag	0.98
Mill scale	0.96

usually used in order to express the degree of oxidation or reduction of a material. A fully oxidized oxygen carrier has a mass conversion degree (ω) of 1. For example, if a material consists of only Fe₂O₃ when fully oxidized, it will have a mass conversion degree of 0.967 when reduced to only Fe₃O₄. Since the oxygen carriers in this work contained not only iron oxides, the reduction degree in Table 2 corresponds to a reduction level beyond the formation of only Fe₃O₄. The theoretical calculation of mass conversion degree has been published previously.¹⁸

To prepare fully oxidized oxygen carriers that would be used as comparison, half of each highly reduced oxygen carrier was calcined once again in the same way as described above. Therewith, each oxygen carrier was obtained in both fully oxidized ($\omega = 1$) and highly reduced state, that is, with mass conversion degree as shown in Table 2. Three potassium salts were used to represent the main ash compounds in biomass, namely potassium carbonate (K₂CO₃), potassium dihydrogen phosphate (KH₂PO₄), and potassium sulfate (K₂SO₄). These salts were manufactured by Sigma AldrichTM, Alfa AesarTM, and MerckTM, respectively, with a purity of more than 99%.

Experimental method

The investigation of interactions between ash substances and oxygen carriers were performed in a horizontal tubular furnace. Two grams of a mixture of a potassium salt and an oxygen carrier was placed in an alumina crucible, which was then put inside the tubular furnace. The amount of the potassium salt in the mixture was adjusted accordingly so that each mixture contained 4 wt.% of potassium, which was chosen based on the amount of accumulated potassium in the bed material of a semi-commercial biomass circulating fluidized bed boiler using ilmenite.²¹ This approach assured that the potassium content was the same in different mixtures even though the total

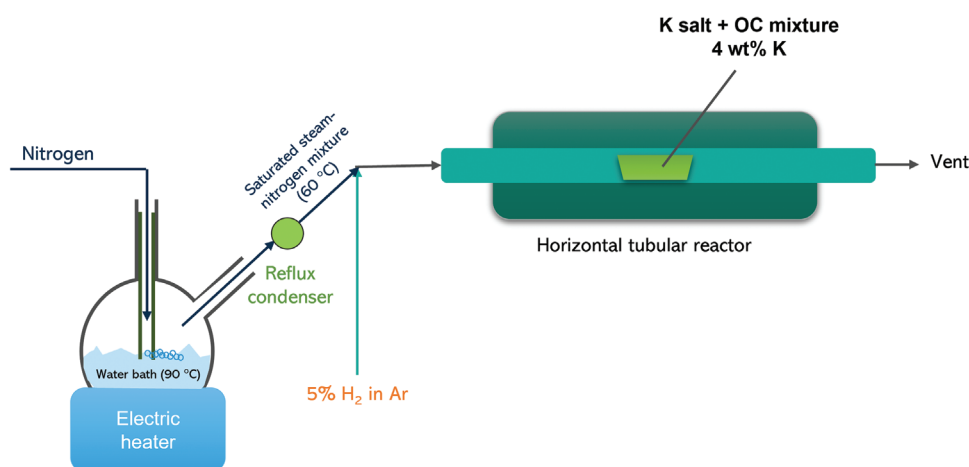


Figure 1. Schematic illustration of the tubular furnace setup used for the performed experiments. The mixture of potassium salt and oxygen carrier was placed in an alumina crucible inside the furnace.

amount of salt varied. Samples of oxygen carrier in both initial oxidation states (reduced and oxidized) without any potassium salt added were also investigated as references. The furnace was heated gradually at a heating rate of 400°C/h to the desired reaction temperature 900°C, which was kept constant for 3 h. Water vapor was generated from a water bath that was heated to 90°C with a constant flow of nitrogen. This steam-nitrogen mixture was then cooled down to 60°C to obtain a saturated flow (50 ml/min 20% steam in N₂) before it was mixed with the diluted hydrogen (50 ml/min 5% H₂ in Ar). See Fig. 1 for schematic representation of the experimental set-up.

This procedure assured that the gas mixture fed into the tubular reactor comprised 2.5% H₂ and 10% steam in Ar and N₂. Using such a gas mixture allowed the salt-oxygen carrier mixture to reach an equilibrium state after the experiment no matter the initial oxidation state of the oxygen carrier (either fully oxidized or highly reduced). In other words, an initially fully oxidized material would be partially reduced, while an initially highly reduced material will be partially oxidized, see Fig. 2.

Characterization and analysis

Each sample was collected after the experiment and characterized. Ocular observation was performed on each sample. The crystalline phases were examined using XRD Bruker D8 Discover, using a copper source with a step size of 0.02° within the 2θ range of 20 – 90°. The XRD characterization was performed to evaluate whether the samples had reached an equilibrium after

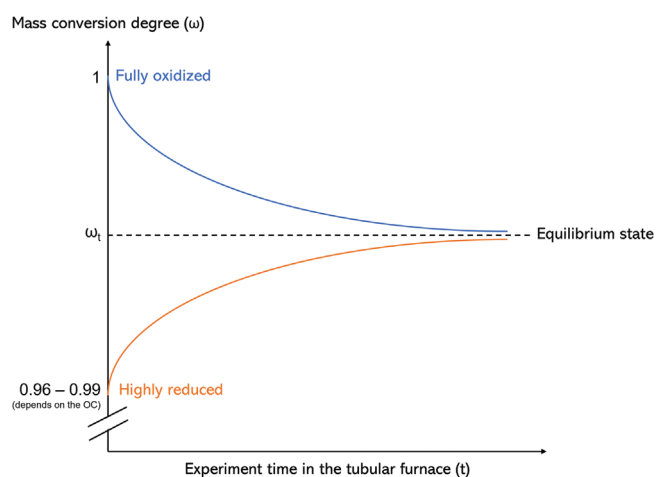


Figure 2. Pathways toward an equilibrium state at a mass conversion degree ω_t from two different initial oxidation states during the experiment in the horizontal tubular reactor.

the experiment in the tubular furnace, independent of the initial redox state. At equilibrium, both the initially fully oxidized and highly reduced oxygen carriers were expected to have the same crystalline phases. Fig. 2 illustrates how the equilibrium state was expected to be reached by an oxygen carrier from two different initial oxidation states during the experiments.

Furthermore, each sample was embedded in epoxy resin and polished to flat cross-section surface prior to the SEM/EDX analysis using JEOL JSM-7800F Prime SEM equipped with an Oxford X-max 80 mm² EDX detector for elemental distribution analysis of the oxygen carrier particles. The used acceleration voltage

was 15 kV and the used signal for imaging was that of backscattered electrons.

Results

Ocular observation upon sample collection

The collected samples from the tubular reactor were characterized ocularly for their degree of agglomeration and change in color. Table 3 shows the summary of the observation results. Here, the basis of the appearance was the corresponding initial state of each sample before the experiment.

Crystalline phase transformation

The crystalline phase transformations of the oxygen carriers, which was analyzed using XRD, were used to show if the equilibrium states have been achieved during the 3-h experiment. The amount of potassium in the mixture (4 wt.%) was at the lower end of the detection limit of the diffractometer, which made it difficult to confirm or exclude the formation of any potassium phase in the samples using XRD. Therefore, the XRD was performed only on the activated and reference samples, which correspond to the oxygen carrier samples without addition of potassium salts before and after experiment, respectively. Table 4 summarizes the crystalline phases detected in these samples. The corresponding diffractograms in Supporting Information Fig. S1 shows that every oxygen carrier forms the same crystalline phases after the experiment independent on the initial redox phase before the experiment (fully oxidized or highly reduced).

Elemental distribution in the oxygen carrier particles

The formed compounds, as a result of the interactions between oxygen carrier particles and potassium salts (used to mimic biomass ashes), were investigated using SEM/EDX. Contrary to the XRD analysis, the focus was the oxygen carrier samples that were mixed with a potassium salt rather than the reference samples. Based on the observations, K from a potassium salt either diffused into the particles, created a layer around the particle, formed interparticle joints between particles, or even followed all the three pathways. The elemental distribution of the samples with potassium salts addition is shown in Figs. 3–6 and the summary of

interactions are summarized in Table 5. The elemental distribution image collection of the activated and reference samples can be found in Supporting Information Figs. S2–S5.

Fig. 3 shows that K from K_2CO_3 and K_2SO_4 diffused into the ilmenite particles' bulk, independent of the initial oxidation states. Meanwhile, K from KH_2PO_4 formed interparticle joints comprising of K and P of which both did not diffuse into the particles' bulk. The joints formed on the surface of the initially highly reduced ilmenite particles appeared to be thicker than that formed on the fully oxidized ones.

In the cases with iron sand, Fig. 4 suggests that K from all three different potassium salts always managed to diffuse into the iron sand particles, independent of the initial oxidation states. Similar to ilmenite, molten phase with K and P enrichment from KH_2PO_4 was formed between iron sand particles no matter what the initial oxidation state was. Furthermore, almost no S from K_2SO_4 was detected in the case of initially highly reduced iron sand.

Fig. 5 visualizes that K from all three different salts formed a layer on the LD slag particle surfaces, except in the case of the mixture comprising initially highly reduced LD slag and K_2SO_4 . In the case of KH_2PO_4 , molten phase with enrichment of K and P was also formed.

As is the case with the other oxygen carriers, it can be seen in Fig. 6 that the addition of KH_2PO_4 caused the formation of K-P-enriched molten phase around the mill scale particles, independent of its initial oxidation state. K from all three potassium salts diffused into the mill scale particle no matter what the initial oxidation state was. In the mixture consisting of initially highly reduced mill scale and K_2CO_3 , a K-enriched layer was also formed around single particles. Enrichment of K and S was also observed in the mixtures comprising K_2SO_4 and mill scale with both initial oxidation states.

Discussion

Based on the XRD results, it can be seen that in the reference case of the oxygen carrier materials, the same phases form in oxidizing and reducing conditions independent of the initial redox phase (fully oxidized or highly reduced). This confirms that an equilibrium state has been reached (as described in Fig. 2). In the case of activated materials, there is a clear distinction between the initial and final redox phases. Fully oxidized oxygen carriers are characterized by the

Table 3. Summary of the ocular observations of the samples, where the agglomeration was classified in three degrees – severe, mild, or none, and the appearance as brighter, darker, or spotty compared to their initial states. FO refers to fully oxidized and HR to highly reduced.

OC	Potassium salt	Initial oxidation state	Physical observation	
			Agglomeration	Appearance
Ilmenite	Reference	FO	None	Same as initial
		HR	None	Same as initial
	K ₂ CO ₃	FO	None	Darker
		HR	None	Same as initial
	KH ₂ PO ₄	FO	Severe	Spotty
		HR	Severe	Brighter
	K ₂ SO ₄	FO	Mild, powdered upon removal	Brighter
		HR	Mild	Brighter
Iron sand	Reference	FO	None	Same as initial
		HR	None	Same as initial
	K ₂ CO ₃	FO	Mild	Darker
		HR	Mild	Same as initial
	KH ₂ PO ₄	FO	Severe	Darker
		HR	Severe	Same as initial
	K ₂ SO ₄	FO	Mild	Spotty
		HR	Mild	Spotty
LD slag	Reference	FO	None	Brighter
		HR	None	Brighter
	K ₂ CO ₃	FO	Mild, powdered upon removal	Brighter
		HR	Mild	Darker
	KH ₂ PO ₄	FO	Mild	Brighter
		HR	Severe	Darker
	K ₂ SO ₄	FO	None	Darker
		HR	Mild	Darker
Mill scale	Reference	FO	Mild, powdered upon removal	Same as initial
		HR	None	Same as initial
	K ₂ CO ₃	FO	Mild, powdered upon removal	Darker
		HR	Mild, powdered upon removal	Brighter
	KH ₂ PO ₄	FO	None	Spotty
		HR	None	Spotty
	K ₂ SO ₄	FO	Mild	Darker
		HR	Mild, powdered upon removal	Brighter

Table 4. The crystalline phases of the studied oxygen carriers in the initially fully oxidized and highly reduced states as detected by XRD analysis. Activated (A) and reference (R) samples correspond to the state of materials without addition of potassium salts before and after the experiment, respectively.

OC	Initial oxidation state	Sample	Crystalline phases
Ilmenite	Fully oxidized	A	Pseudobrookite (Fe_2TiO_5) Hematite (Fe_2O_3) Rutile (TiO_2)
		R	Titanium iron oxide ($\text{Ti}_x\text{O}_{2-x}\text{O}_3$ or $\text{Ti}_y\text{O}_{3-y}\text{O}_4$) Rutile (TiO_2)
	Highly reduced	A	Titanium iron oxide ($\text{Ti}_x\text{Fe}_{2-x}\text{O}_3$ or $\text{Ti}_y\text{Fe}_{3-y}\text{O}_4$) Elemental iron (Fe) Rutile (TiO_2)
		R	Titanium iron oxide ($\text{Ti}_x\text{Fe}_{2-x}\text{O}_3$ or $\text{Ti}_y\text{Fe}_{3-y}\text{O}_4$) Rutile (TiO_2)
Iron sand	Fully oxidized	A	Hematite (Fe_2O_3) Magnetite (Fe_3O_4)
		R	Magnetite (Fe_3O_4) Fayalite (Fe_2SiO_4)
	Highly reduced	A	Magnetite (Fe_3O_4) Wüstite (FeO) Clinoferrosilite (FeSiO_3)
		R	Magnetite (Fe_3O_4) Fayalite (Fe_2SiO_4)
LD slag	Fully oxidized	A	Hematite (Fe_2O_3) Magnetite (Fe_3O_4) Lime (CaO) Larnite (Ca_2SiO_4) Calcium iron oxide ($\text{Ca}_2\text{Fe}_2\text{O}_5$)
		R	Wüstite (FeO) Lime (CaO) Larnite (Ca_2SiO_4) Calcium iron oxide ($\text{Ca}_2\text{Fe}_2\text{O}_5$)
	Highly reduced	A	Wüstite (FeO) Elemental iron (Fe) Lime (CaO) Larnite (Ca_2SiO_4) Calcium iron oxide ($\text{Ca}_2\text{Fe}_2\text{O}_5$)
		R	Wüstite (FeO) Lime (CaO) Larnite (Ca_2SiO_4) Calcium iron oxide ($\text{Ca}_2\text{Fe}_2\text{O}_5$)
	Fully oxidized	A	Hematite (Fe_2O_3)
		R	Magnetite (Fe_3O_4) Wüstite (FeO)
Mill scale	Fully oxidized	A	Hematite (Fe_2O_3)
		R	Magnetite (Fe_3O_4) Wüstite (FeO)
	Highly reduced	A	Magnetite (Fe_3O_4) Wüstite (FeO)
		R	Magnetite (Fe_3O_4) Wüstite (FeO)

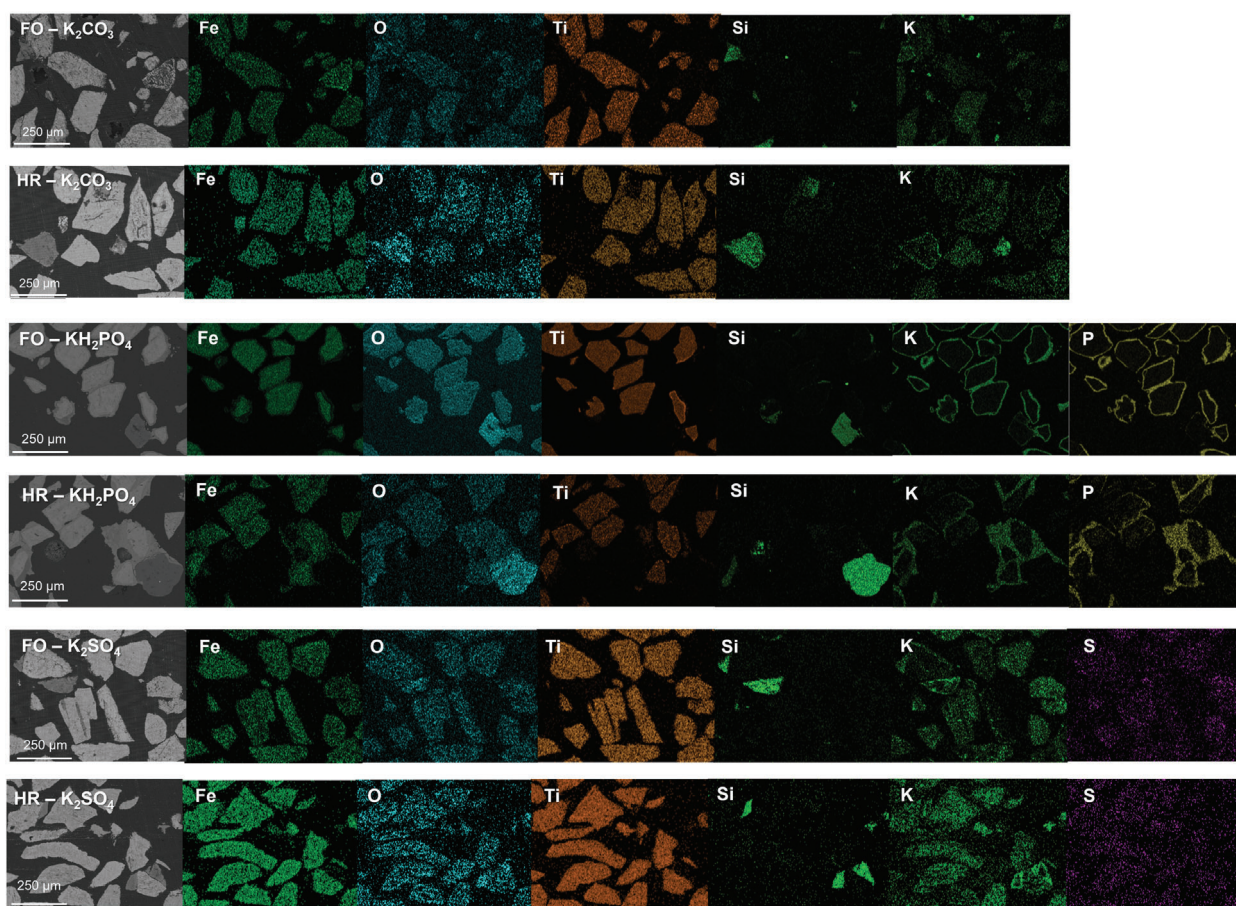


Figure 3. Elemental distribution of ilmenite samples with potassium salts addition observed using SEM/EDX analysis. FO and HR refer to fully oxidized and highly reduced, respectively.

presence of iron in its most oxidized state as 3+ (e.g., Fe_2O_3 , hematite). On the other hand, the highly reduced ones comprise either Fe in a reduced state as 2+ (Fe_3O_4 , magnetite, and/or FeO , wüstite) or 0 as metallic iron (Fe). These findings suggest that the experiment allows to reach the expected equilibrium state.

The interactions between an iron-based oxygen carrier and a potassium salt are based on both ocular observations as presented in the ocular observation upon sample collection section and SEM/EDX results as described in the elemental distribution in the oxygen carrier particles section. The discussion can be broken down to several subjects as follows:

Effect of the type of potassium salt

According to the potassium distribution seen from the SEM/EDX results, the K from K_2CO_3 and K_2SO_4 tends to diffuse into the oxygen carrier particles' bulk, while the K originating from KH_2PO_4 always formed a

distinct layer around the particle and in most cases created interparticle joints, which contributed to the agglomeration of the particles (see Table 3). This observation was valid for all the examined oxygen carriers. The exception to this was mill scale, which did not experience any observable agglomeration with KH_2PO_4 , even though the SEM/EDX images indicate the formation of interparticle joints (see Fig. 6). This could indicate that the interparticle joints formed between K from KH_2PO_4 and initially high reduced mill scale did not lead to significant particle aggregation as they occurred on only limited spots. Perhaps, this is partially due to the penetration of K and P into the mill scale's bulk, making K unavailable for melt formation and further agglomeration.

Effect of the oxygen carrier surface

Furthermore, the type of the oxygen carrier material surface itself contributes to the interaction with the

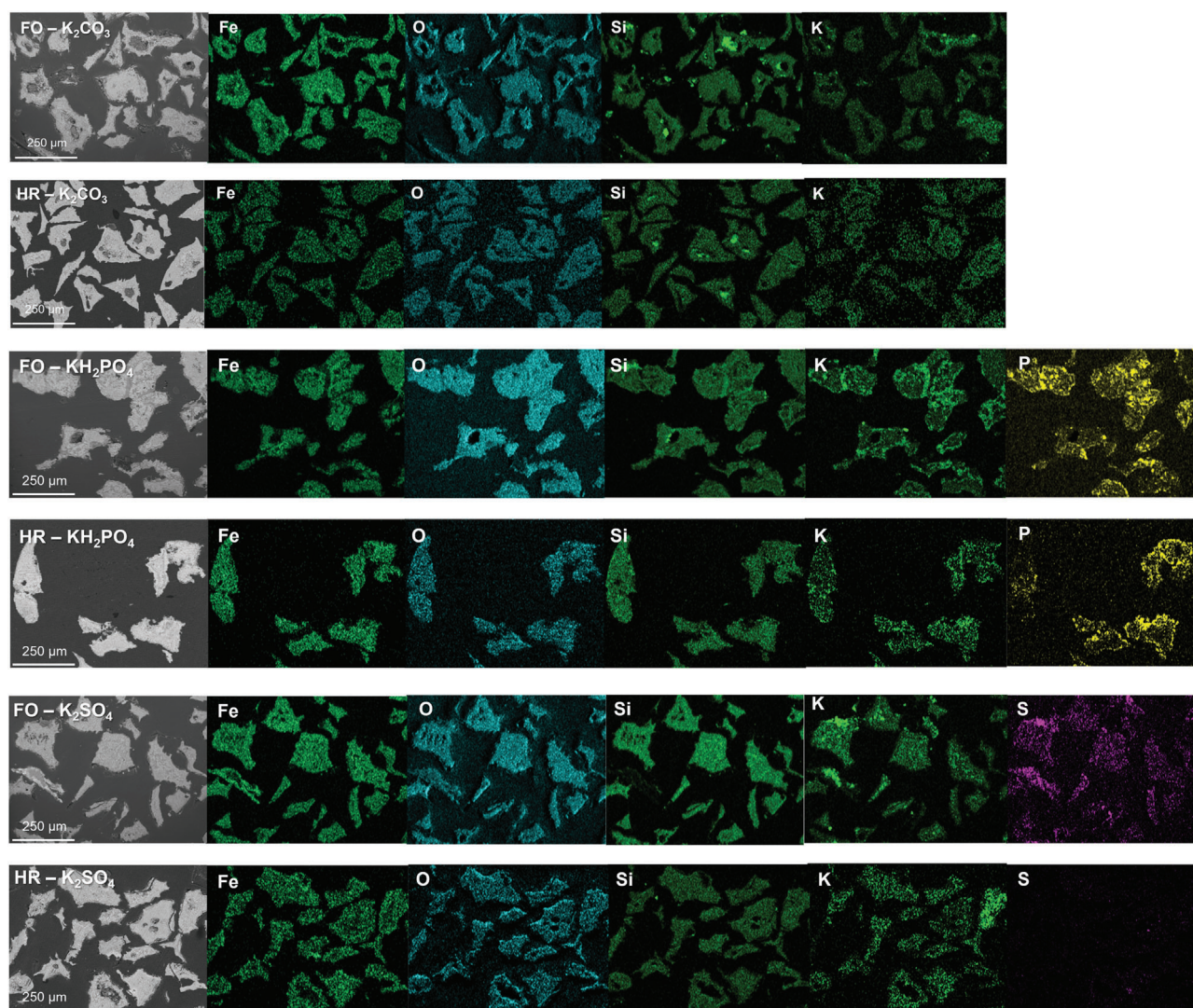


Figure 4. Elemental distribution of iron sand samples with potassium salts addition observed using SEM/EDX analysis. FO and HR refer to fully oxidized and highly reduced, respectively.

chosen potassium salt. Among the tested materials it can be clearly seen that iron sand always showed a certain extent of agglomeration after being exposed to any potassium salt, while mill scale did not experience any severe agglomeration at all, no matter the chosen salt. This observation can be explained by the difference in the content of silicon (Table 1) where iron sand has four times higher content of silicon than mill scale. The rich content of silica in iron sand may contribute to its agglomeration, since silicon and potassium can easily attract each other¹⁰ to form potassium silicate, which has a low melting point.²² The case with mill scale, on the other hand, suggested that the iron content alone (95 wt.%, according to

Table 1) in an oxygen carrier material is less likely to cause severe agglomeration on the whole material bed despite the presence of a few percent of silicon (observe that mill scale has higher content of silicon than ilmenite). The mild agglomeration on the mill scale – K_2SO_4 mixture (Table 3 and Fig. 6) suggested that the presence of S within the particle bulk can trigger the formation of interparticle joints. This phenomenon can likely be explained with the formation of low melting sulphate phases on the surface of the particles that can act as initiators of agglomeration. Since materials have been collected after cooling, it is difficult to interpret what the effect of cooling has been on the formed interparticle joints and how it has affected the degree of

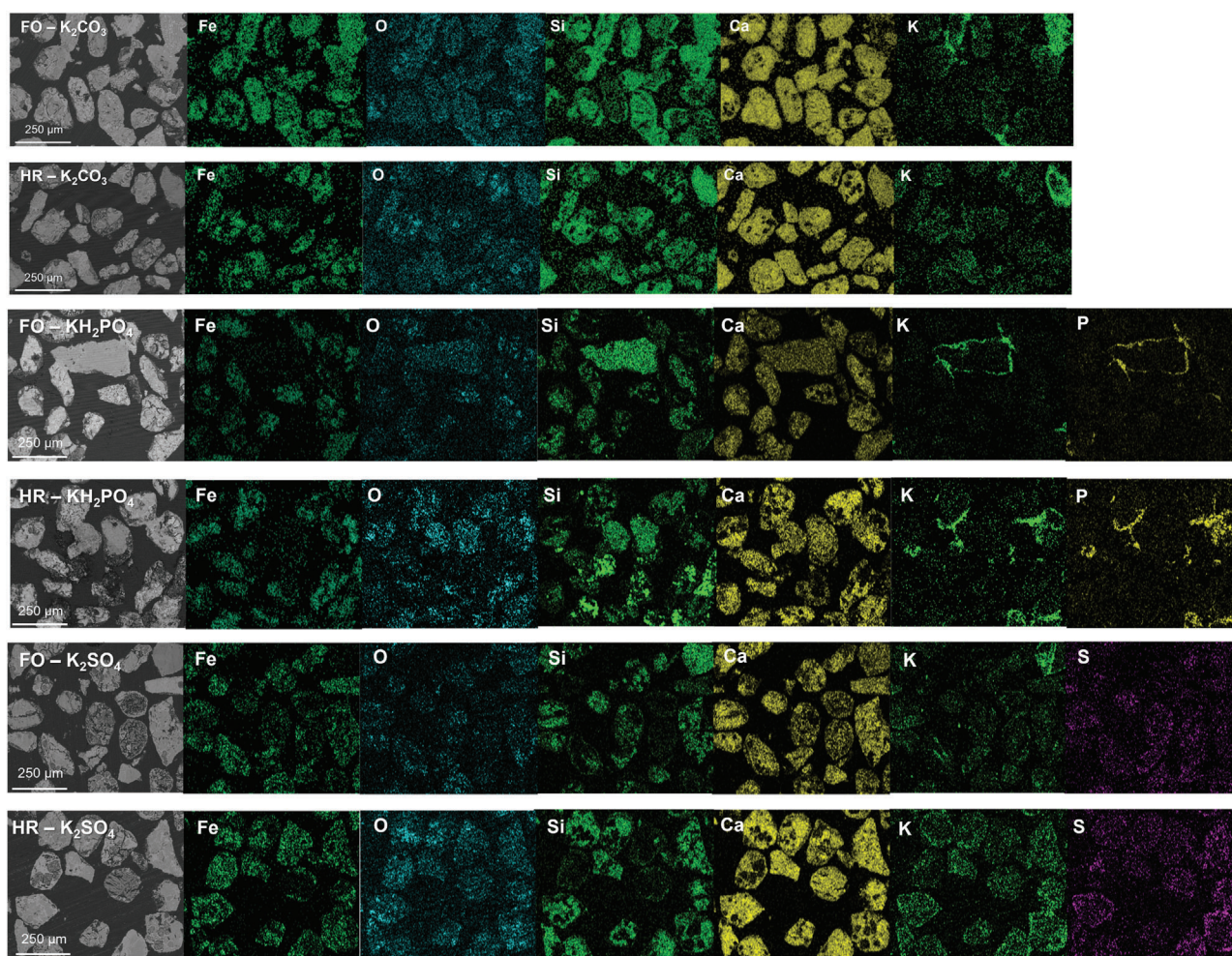


Figure 5. Elemental distribution of LD slag samples with potassium salts addition observed using SEM/EDX analysis. FO and HR refer to fully oxidized and highly reduced, respectively.

agglomeration. Further studies are therefore necessary to investigate this phenomenon.

Effect of the initial oxidation state of the oxygen carrier on K interactions

Lastly, the initial oxidation state of the oxygen carrier material can affect the interaction between the material and the chosen potassium salt. This can mainly be due to the chemical phases that are formed on the particles' surface.

The K-P layers on both ilmenite- KH_2PO_4 samples (with different initial oxidation states) suggest the possible formation of a molten phase on the surface of ilmenite particles. The formed phase on the initially highly reduced ilmenite is more pronounced than that

on the initially fully oxidized one (see Fig. 3). On the other hand, the initial oxidation state of ilmenite barely affected the interactions between the material and K_2CO_3 and K_2SO_4 , which above all involved a mere diffusion of K into the particle bulks. This suggests that the effect is a result of a combination of initial redox state of the oxygen carrier and type of salt rather than a sole effect of the former. The lack of interaction between ilmenite surface and either K_2CO_3 or K_2SO_4 is in agreement with previously published study in which no agglomeration was detected when ilmenite was mixed with both potassium salts under similar conditions.²²

Even though suggesting the same effect as in the case of ilmenite, the mechanism behind interaction of iron sand and K_2SO_4 was different. In the case of highly

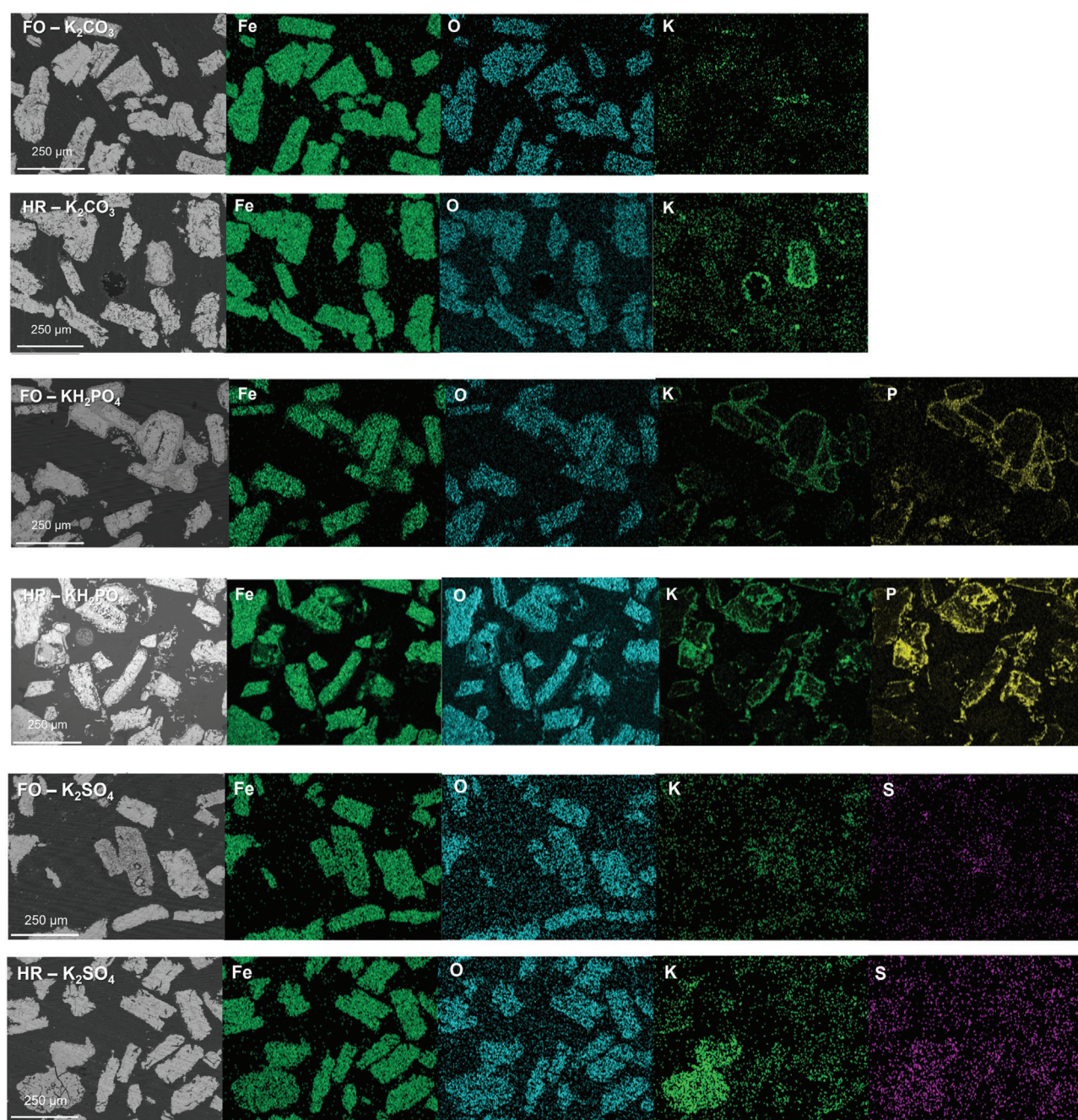


Figure 6. Elemental distribution of mill scale samples with potassium salts addition observed using SEM/EDX analysis. FO and HR refer to fully oxidized and highly reduced, respectively.

reduced iron sand – K_2SO_4 mixture, barely any S element was detected under the surface. This indicates that S might have left the system in the form of H_2S and SO_2 gases due to the presence of steam.³ This is supported by the color change of the water in the gas washing bottle in the outlet from transparent to yellow. Furthermore, the water had a sulfuric smell

when disposed. Still, mild agglomeration was observed on both initially fully oxidized and highly reduced iron sand – K_2SO_4 mixtures, so whether S diffused into the material bulks or not, did not significantly affect the physical characteristics of the mixture.

While there were K-S-enriched layers on the particle surface in initially highly reduced LD slag – K_2SO_4

Table 5. Summary of interactions between oxygen carrier and K from potassium salts as observed using SEM/EDX mapping.

OC	Potassium salt	Initial oxidation state*	Type of interaction between K and oxygen carrier**		
			Diffusion	Layer	Joint
Ilmenite	K_2CO_3	FO	Yes	No	No
		HR	Yes	Yes, around an SiO_2 particle	No
	KH_2PO_4	FO	No	Yes (+P)	Yes
		HR	No	Yes (+P), thicker than FO	Yes
	K_2SO_4	FO	Yes	Yes, around an SiO_2 particle	No
		HR	Yes	Yes, around an SiO_2 particle	No
Iron sand	K_2CO_3	FO	Yes	No	No
		HR	Yes	No	No
	KH_2PO_4	FO	Yes	Yes (+P)	Yes
		HR	Yes	Yes (+P)	Yes
	K_2SO_4	FO	Yes (+S)	No	No
		HR	Yes, but barely any S detected in the sample	No	No
LD slag	K_2CO_3	FO	Yes	No	Yes
		HR	Yes	No	No
	KH_2PO_4	FO	No	Yes (+P)	Yes, around an Si – Mg – O particle
		HR	No	Yes (+P)	Yes
	K_2SO_4	FO	Yes	No	No
		HR	Yes	Yes (+S)	No
Mill scale	K_2CO_3	FO	Yes	No	No
		HR	Yes	Yes	No
	KH_2PO_4	FO	No	Yes (+P)	Yes (+P)
		HR	Yes	Yes (+P)	Yes (+P)
	K_2SO_4	FO	Yes	Yes	No
		HR	Yes	Yes	No

*Abbreviations: FO – fully oxidized, HR – highly reduced.

**(+X) indicates that element X is present at the same location with K.

mixture, which contributed to the mild agglomeration of the mixture, the same effect was not observed on the initially fully oxidized one. This can be due to preferential enrichment of S on the surface of the initially highly reduced LD slag compared to the

initially fully oxidized one, where S is more enriched in the particles' bulk, see Fig. 5. Hence, the initial oxidation states of LD slag may affect the interactions between the material and K_2SO_4 , at least in a fixed bed system.

Table 6. Summary of possible mechanisms of interactions between oxygen carriers' surface and potassium salts. FO and HR refer to fully oxidized and highly reduced, respectively.

OC	Potassium salt	Initial oxidation state	Possible mechanism
Ilmenite	K_2CO_3	FO	Barely any interaction
		HR	
	KH_2PO_4	FO	Formation of K-P-enriched molten phase
		HR	
	K_2SO_4	FO	Barely any interaction
		HR	
Iron sand	K_2CO_3	FO	Barely any interaction
		HR	
	KH_2PO_4	FO	Formation of K-P-enriched molten phase
		HR	
	K_2SO_4	FO	Barely any interaction
		HR	
LD slag	K_2CO_3	FO	Formation of K layer on several spots
		HR	
	KH_2PO_4	FO	Formation of K-P-enriched molten phase
		HR	
	K_2SO_4	FO	Barely any interaction
		HR	
Mill scale	K_2CO_3	FO	Barely any interaction
		HR	
	KH_2PO_4	FO	Formation of K-P-enriched molten phase
		HR	
	K_2SO_4	FO	Enrichment of K and S on particles' surface
		HR	

It seems that the initial oxidation states of mill scale did not substantially affect the interaction between the material and any of the potassium salts, which is not unexpected since, as mentioned above, the high iron content in the material may have hindered further interactions between the mill scale particles and potassium.

The mechanisms behind interactions between oxygen carriers' surface and the potassium salts are summarized in Table 6.

Conclusions

Biomass-based chemical looping processes has developed into several technologies which require less oxygen, such as chemical looping gasification. As the development continues forward it is essential to study how the major ash compounds in biomass may affect a highly reduced oxygen carrier surface. The benchmark natural-ore-based oxygen carrier, ilmenite, and three waste-based material, namely iron sand, LD slag, and mill scale, were prepared in a highly reduced state. Each oxygen carrier was mixed with one of three different potassium salts: K_2CO_3 , KH_2PO_4 , and K_2SO_4 , and exposed to a slightly reducing condition (2.5% H_2 and 10% steam in Ar and N_2) at 900°C for 3 h. It was found that both initially fully oxidized and highly reduced material ended up having the same crystalline phases post-experiment.

The results suggest that both the type of potassium salt and oxygen carrier initial redox state involved in the experiments affect such an interaction significantly. In most cases, K_2CO_3 and K_2SO_4 tend to diffuse into the particles' bulk, while KH_2PO_4 always forms a layer surrounding the particle surface. Iron sand always shows certain extents of agglomeration upon interaction with any potassium salt, while mill scale is generally the least prone to agglomeration among all.

The initial oxidation state of an oxygen carrier was found to affect the chemical phases on the oxygen carrier's surface and, therefore, interactions between the material and a potassium salt to certain extents. Nevertheless, it should be noted that the final state of the mixtures postexperiment is less affected by such an effect. LD slag was an exception since its initially highly reduced form did agglomerate partially upon interaction with K_2SO_4 , which can be due to the enrichment of S on its surface compared to the initially fully oxidized one. Since the interactions between an oxygen carrier and a chosen potassium salt are similar in both samples with different initial oxidation states, the initial oxidation state on the oxygen carriers' surface likely plays a minor role in affecting the interactions themselves.

Acknowledgments

This work was funded by Stiftelsen ÅForsk (20-269) and Swedish Energy Agency (Project 51430-1). The ilmenite and iron sand in this study were provided by Titania A/S and Boliden AB, respectively. SSAB

(Swedish Steel) is acknowledged for providing the LD slag and mill scale. The authors acknowledge Elin Strömberg, Emma Albinsson, Frida Törnqvist, Hampus Dahlberg, Hanna Pettersson, and Jessika Öhberg for performing parts of experimental work in this study as a student project.

Nomenclatures

AR	Air reactor
CCUS	Carbon capture and storage
CLG	Chemical looping gasification
EDX	Energy-dispersive X-ray spectroscopy
FR	Fuel reactor
FO	Fully oxidized
HR	Highly reduced
LD	Linz-Donawitz
OC	Oxygen carrier
OCAC	Oxygen-carrier-aided combustion
SEM	Scanning electron microscopy
XRD	X-ray diffraction

References

1. Abdalla A, Mohamedali M, Mahinpey N. Recent progress in the development of synthetic oxygen carriers for chemical looping combustion applications. *Catal Today*. 2022;407:21–41. <https://doi.org/10.1016/j.cattod.2022.05.046>.
2. Yu Z, Yang Y, Yang S, Zhang Q, Zhao J, Fang Y, et al. Iron-based oxygen carriers in chemical looping conversions: A review. *Carbon Resour Convers*. 2019;2:23–34.
3. Hildor F, Zevenhoven M, Brink A, Hupa L, Leion H. Understanding the interaction of potassium salts with an ilmenite oxygen carrier under dry and wet conditions. *ACS Omega*. 2020;5:22966–77.
4. Leion H, Lyngfelt A, Johansson M, Jerndal E, Mattisson T. The use of ilmenite as an oxygen carrier in chemical-looping combustion. *Chem Eng Res Des*. 2008;86:1017–26.
5. Störner F, Lind F, Rydén M. Oxygen carrier aided combustion in fluidized bed boilers in Sweden—review and future outlook with respect to affordable bed materials. *Appl Sci*. 2021;11:7935.
6. Purnomo V, Yilmaz D, Leion H, Mattisson T. Study of defluidization of iron- and manganese-based oxygen carriers under highly reducing conditions in a lab-scale fluidized-bed batch reactor. *Fuel Process Technol*. 2021;219:106874.
7. Purnomo V, Staničić I, Mattisson T, Rydén M, Leion H. Performance of iron sand as an oxygen carrier at high reduction degrees and its potential use for chemical looping gasification. *Fuel*. 2023;339. <https://doi.org/10.1016/j.fuel.2022.127310>
8. Coppola A, Scala F. Chemical looping for combustion of solid biomass: a review. *Energy and Fuels*. 2021;35:19248–65.
9. Staničić I, Hanning M, Deniz R, Mattisson T, Backman R, Leion H, et al. Interaction of oxygen carriers with common biomass ash components. *Fuel Process Technol*. 2020;200:106313.
10. Staničić I, Mattisson T, Backman R, Cao Y, Rydén M. Oxygen carrier aided combustion (OCAC) of two waste fuels - Experimental and theoretical study of the interaction between ilmenite and zinc, copper and lead. *Biomass Bioenergy*. 2021;148:106060.
11. Eliason F. Ash interactions with oxygen carriers Glödsdal and LD-slag in biomass-CLC. Master's thesis. Gothenburg, Sweden; Chalmers University of Technology; 2018.
12. Störner F, Hildor F, Leion H, Zevenhoven M, Hupa L, Rydén M, et al. Potassium ash interactions with oxygen carriers steel converter slag and iron mill scale in chemical-looping combustion of biomass-experimental evaluation using model compounds. *Energy Fuels*. 2020;34:2304–14.
13. Yilmaz D, Steenari BM, Leion H. Comparative study: impacts of Ca and Mg salts on iron oxygen carriers in chemical looping combustion of biomass. *ACS Omega*. 2021;6(25):16649–60. <https://doi.org/10.1021/acsomega.1c02138>.
14. Cheng D, Yong Q, Zhao Y, Gong B, Zhang J. Study on the interaction of the Fe-based oxygen carrier with ashes. *Energy Fuels*. 2020;34:9796–809.
15. Rubel A, Zhang Y, Liu K, Neathery J. Effet des cendres sur l'activité des porteurs d'oxygène dans la combustion du charbon en boucle chimique to a high carbon char [Effect of ash on oxygen carriers for the application of chemical looping combustion]. *Oil Gas Sci Technol*. 2011;66:291–300.
16. Bao J, Li Z, Cai N. Promoting the reduction reactivity of ilmenite by introducing foreign ions in chemical looping combustion. *Ind Eng Chem Res*. 2013;52:6119–28.
17. Vigoureux M, Leffler T, Knutsson P, Lind F. Sulfur capture and release by ilmenite used as oxygen carrier in biomass combustor. *Fuel*. 2022;309:121978.
18. Hildor F, Leion H, Linderholm CJ, Mattisson T. Steel converter slag as an oxygen carrier for chemical-looping gasification. *Fuel Process Technol*. 2020;210:106576.
19. Leion H, Frick V, Hildor F. Experimental method and setup for laboratory fluidized bed reactor testing. *Energies*. 2018;11:2505.
20. Schwebel GL, Sundqvist S, Krumm W, Leion H. Apparent kinetics derived from fluidized bed experiments for Norwegian ilmenite as oxygen carrier. *J Environ Chem Eng*. 2014;2:1131–41.
21. Corcoran A, Marinkovic J, Lind F, Thunman H, Knutsson P, Seemann M, et al. Ash properties of ilmenite used as bed material for combustion of biomass in a circulating fluidized bed boiler. *Energy Fuels*. 2014;28:7672–9.
22. Hildor F, Yilmaz D, Leion H. Interaction behavior of sand-diluted and mixed Fe-based oxygen carriers with potassium salts. *Fuel*. 2022;339:127372.



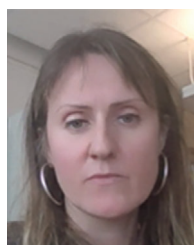
Victor Purnomo

Victor Purnomo is PhD student at the Department of Chemistry and Chemical Engineering, Chalmers University of Technology in Gothenburg, Sweden. His works cover investigation of ore- and waste-based oxygen carriers under highly reducing atmosphere, which is relevant for chemical looping gasification.



Fredrik Hildor

Fredrik Hildor is doctoral student at Chalmers University of Technology in Gothenburg, Sweden. His works cover the investigation of steel converter slag as an oxygen carrier in high temperature fuel conversion processes, such as chemical looping combustion and oxygen carrier aided combustion.



Pavleta Knutsson

Dr Pavleta Knutsson is associate professor at Chalmers University of Technology in Gothenburg, Sweden. Her expertise is in surface chemistry, catalytic activation of materials in high temperature fuel conversion processes in fluidized bed, and material characterization.



Henrik Leion

Dr Henrik Leion is professor at the Department of Chemistry and Chemical Engineering, Chalmers University of Technology in Gothenburg, Sweden. His expertise is in the investigation of oxygen carriers and chemical reactions between fuels and oxygen carriers in chemical looping combustion.